

## SPECTRAL BEHAVIOR OF THE LUNAR OPPPOSITION EFFECT FROM THE CHANDRAYAAN-1 M<sup>3</sup>

**DATA.** V. Kaydash<sup>1</sup>, C. Pieters<sup>2</sup>, Y. Shkuratov<sup>1</sup>, V. Korokhin<sup>1</sup>, M. Stepaniuk<sup>1</sup>, Astronomical Institute of V. N. Karazin Kharkov National University, 35 Sumskaya Street, Kharkov 61022, Ukraine, vgkaydash@gmail.com,  
<sup>2</sup>Department of Geological Sciences, Brown University, Providence 02912, RI, USA, carle\_pieters@brown.edu.

**Introduction:** The actual proportions of the shadow-hiding (SH) and coherent backscattering enhancement (CBE) mechanisms to the brightness opposition effect (OE) of the Moon at different phase angles still remain not well determined [1, 2]. In order to estimate the relative contributions of these effects we calculated phase functions of apparent reflectance and color-ratios for several mare and highland sites [3]. We utilize imaging spectrometer data acquired by the Moon Mineralogy Mapper (M<sup>3</sup>) onboard Chandrayaan-1 spacecraft [4]. We study changes in the wavelength dependence of the reflectance phase curves  $f(\alpha)$  at small phase angles  $\alpha$  and interpret them in terms of different effects dominating the lunar OE.

**Processing of M<sup>3</sup> data used:** We use M<sup>3</sup> spectra measured with 20-40 nm sampling and processed with a sequence of algorithms applied to calibrate downlinked data spectrally, radiometrically, and spatially [5, 6]. In the current study we focus on M<sup>3</sup> images with the opposition geometry (i.e. at  $\alpha \sim 0$ ). To correct the digital numbers in M<sup>3</sup> images for the photometric properties of the lunar surface we applied the Lommel-Seeliger terminator-darkening factor. We here show a result that is representative for the study [3]. Figure 1 displays a fragment of the image M3G20090611T090220 of mare area in a south-eastern portion of Oceanus Procellarum near the craters Encke B and C. The center of the diffuse latitudinally elongated spot in the reflectance image corresponds to zero-phase-angle point. The longitudinal width of the image is 304 pixels, which corresponds to 85 km swath. To retrieve phase functions near opposition from M<sup>3</sup> lunar orbit imaging we take into account the substantial  $\alpha$  variation in a single scene (Fig. 1). We applied a simple averaging of apparent reflectances over image in concentric elliptical bins of constant phase angles. When averaging the reflectance we have masked mare and highland craters, low reflectance areas (in case of highland sites), and bright features for mare sites (see [3] for detail).

**Spectral behavior of OE amplitude:** There are totally 83 usable spectral bands from 540.84 to 2976.2 nm with a spectral resolution of 20 nm for bands from 730 nm to 1548 nm and 40 nm for other spectral ranges. We calculated phase curves for all the 83 bands. Phase curves are sampled in every  $0.3^\circ$  with a bin width of  $0.3^\circ$ .

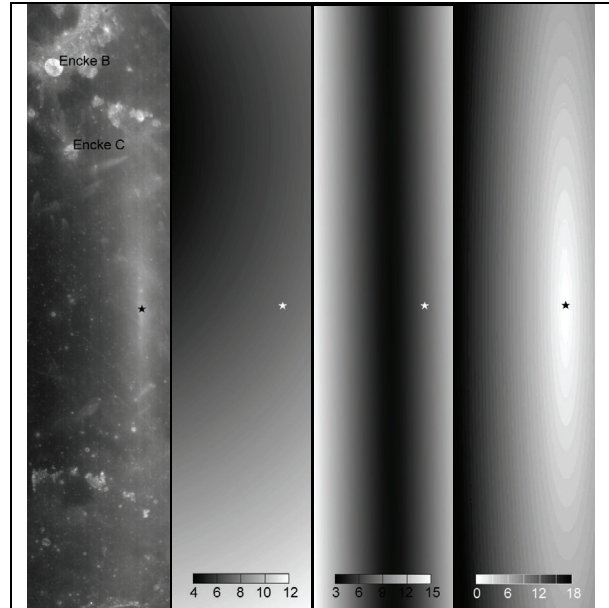


Figure 1. A distribution of photometric angles over the part of the M<sup>3</sup> image. Left to right: apparent reflectance at 1489 nm, incidence, emission, and phase angle. Angle ranges in degrees are shown in scale bars. Zero-phase-angle point is marked with star. North is up.

**Normalized phase function:** Figure 2 shows reflectance phase curves at different wavelengths  $\lambda$ . Residual variability in the M<sup>3</sup> detector response [6] and real albedo variations over scenes results in some noise on the final phase curves, and can be seen as false details of phase functions simultaneously in all spectral bands. Nevertheless derived phase functions reveals an inverse wavelength dependence of their steepness: the slope of phase function is greater for shorter wavelength. The phase ratio  $f(0.15^\circ)/f(10^\circ)$  is about 1.5 for the scene in Fig. 1.

**Phase curve of color-ratio.** A non-monotonic behavior of phase curves of color-ratios  $C(\alpha) = f(\lambda_1, \alpha)/f(\lambda_2, \alpha)$ ,  $\lambda_1 > \lambda_2$  in visible spectral interval (colorimetric OE) was noted using laboratory measurements of lunar regolith samples [1]. The phase reddening (increasing the  $C(\alpha)$  when  $\lambda_1 > \lambda_2$  with  $\alpha$ ) is well-known while the minimum of the function  $C(\alpha)$  was never confirmed with lunar orbital photometry. Using the M<sup>3</sup> multispectral data we calculated functions  $C(\alpha)$ ,  $\lambda_1 = 540.84-2976.2$ ,  $\lambda_2 = 540.84$  nm. The phase curves reveal a clear minimum of  $C(\alpha)$  (Fig.

3). At wavelengths below 1000 nm a very shallow minimum at 4–6° (or no minimum at all) can be seen. For  $\lambda > 1000$  nm this minimum is pronounced and located at 2–4°.

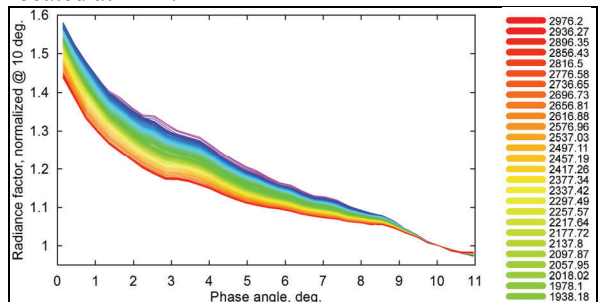


Figure 2. Phase functions for the area shown in Fig. 1. Each curve is normalized on its own value at  $\alpha=10^\circ$ . For the rainbow-style color coding all 83 curves from the wavelength range 541–2976 nm are used.

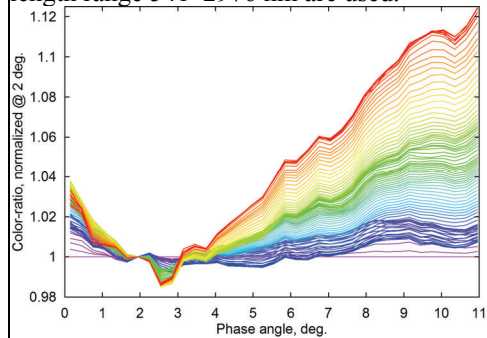


Figure 3. Phase dependences of color-ratio  $C(\alpha) = A(\lambda_1, \alpha)/A(\lambda_2, \alpha)$ , where  $\lambda_2 = 540.84$  nm, for the area shown in Fig. 1. Each curve is normalized on its own value at  $\alpha = 2^\circ$ .

**Discussion:** To clarify the role of the CBE in the formation of the phase function we calculated several phase ratios and plotted them as a function of wavelength  $\lambda$  (Fig. 4). We choose these ratios because the nonlinear increase of the reflectance related to the CBE begins with  $\alpha \sim 5^\circ$ . Thus we consider the phase ratios  $f(0.15^\circ)/f(1^\circ)$  and  $f(2^\circ)/f(3^\circ)$  as an assessment of the enhancement. The phase-ratio  $f(0.15^\circ)/f(1^\circ)$  plot reveal an increase of the phase slope with  $\lambda$ . Such a behavior means that the OE amplitude in the range 0–1° tends to increase with albedo in spite of the reverse influence of incoherent multiple scattering (IMS). Thus, the wavelength dependence of the ratio  $f(0.15^\circ)/f(1^\circ)$  is clear evidence that the CBE becomes important for the Moon at  $\alpha < 1–2^\circ$  for  $\lambda$  from 541 to 2976 nm. The phase ratio  $f(2^\circ)/f(3^\circ)$  is almost constant  $\sim 1$  over the whole wavelength range, i.e. at the 2–3° the phase function slope does not depend on  $\lambda$ . In this case the contributions of the CBE and IMS equalize each other. This points out that the spike due to CBE is

somewhat wider than 1°. Phase ratios  $f(5^\circ)/f(7^\circ)$  and  $f(6^\circ)/f(10^\circ)$  decrease with  $\lambda$ . Hence we confirm an inverse wavelength (albedo) dependence of the steepness of phase curves at the  $\alpha=5–10^\circ$  [1]. Thus we may conclude that SH and IMS are the major components of light scattering at  $\alpha > 2^\circ$  even in NIR. This is in sharp contrast to the conclusion by Hapke et al. [7] who suggested that the CBE contributes nearly 40% in the UV, increasing to over 60% in the red. A minimum of  $C(\alpha)$  at  $\alpha = 2–4^\circ$  is caused rather by the CBE which values do not exceed 5–7% even in NIR spectrum range.

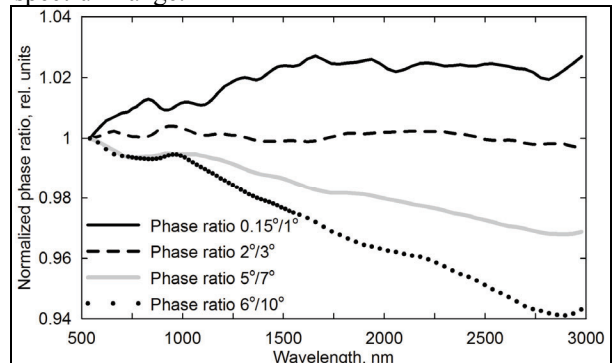


Figure 4. Phase-angle ratios,  $f(0.15^\circ)/f(1^\circ)$ ,  $f(2^\circ)/f(3^\circ)$ ,  $f(5^\circ)/f(7^\circ)$ , and  $f(6^\circ)/f(10^\circ)$  plotted as a function of wavelength for the area from Fig. 1. Phase ratios are normalized to their own values at 541 nm.

**Conclusion:** We suggest a new description of the wavelength dependence of lunar OE in the range 541–2976 nm. We interpret derived phase curves as evidence of dominating SH and IMS in the OE at  $\alpha > 1–2^\circ$ . At  $\alpha < 1–2^\circ$  the CBE may also contribute to scattering, however, its values is rather small, 5–7% even at  $\lambda = 3 \mu\text{m}$ , where lunar surface albedo is rather high. Our results reveal the colorimetric OE of the Moon in NIR. Using lunar observations, this is first reliable evidence of the colorimetric OE found earlier for samples. We found a minimum of phase functions of color-ratio at  $\alpha_{\min} \sim 2–4^\circ$  which would be considered as the first reliable indicator of a small CBE component at  $\alpha < 1–2^\circ$ .

**References:** [1] Shkuratov Y. et al. (2011) *Planet. Space Sci.*, 59, 1326–1371. [2] Shkuratov Y. G. et al. (2012) *Journ. Quant. Spectrosc. Rad. Transfer*, 113, 2431–2456. [3] Kaydash V. et al. (2013) *JGR Planets*, submitted. [4] Pieters C. M. et al. (2009) *Current Science*, 96, 500–505. [5] Lundein S. et al (2011) [http://pds-imaging.jpl.nasa.gov/data/m3/CH1M3\\_0004/DOCUMENT/DPSIS.PDF](http://pds-imaging.jpl.nasa.gov/data/m3/CH1M3_0004/DOCUMENT/DPSIS.PDF). [6] Crean R. O. et al. (2011) *JGR Planets*, 116, E00G19, doi:10.1029/2011JE003797. [7] Hapke B. et al. (2012) *JGR Planets*, 117, E00H15, doi:10.1029/2011JE003916.